



Connectivity in Wireless Sensor Networks

LI Yanjun

June 16, 2008 internal presentation



Outline

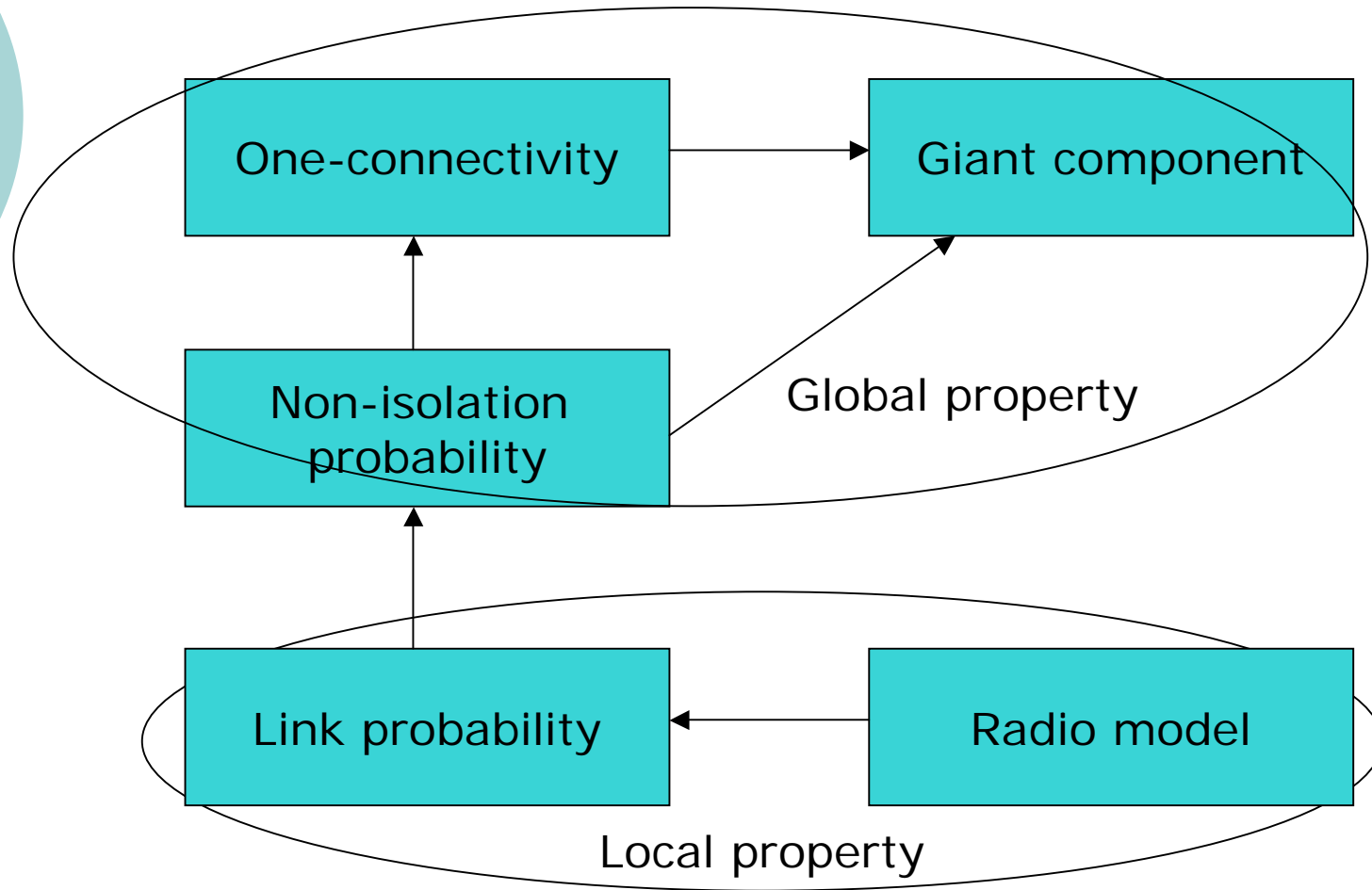
- Introduction and motivation
- Connectivity analysis
- Link probability analysis
- Simulation results
- Conclusion and future work



Introduction and motivation

- Connectivity is a fundamental property and provides design reference for upper-layer protocols.
- Boolean disk model is too simple, real wireless channel is dynamic, with path loss, fading and shadowing.
- Investigate connectivity under more realistic channel model, study how various parameters impact the quality of connectivity.

Main idea





Connectivity analysis

- Node spatial distribution—homogenous Poisson point process

$N(A, \cdot)$ is the number of nodes in subarea A which follows Poisson distribution with mean $\lambda(A)$:

$$P(N(A) = k) = \frac{\lambda(A)^k}{k!} e^{-\lambda(A)}, \text{ all } A \in \mathcal{F}, \quad (1)$$

with an expected value $E(N) = \lambda(A) = \rho(A)\|A\|$, ρ and $\|A\|$ are node density and size of subarea A respectively.

If A_1, A_2, \dots are disjoint sets then $N(A_1, \cdot), N(A_2, \cdot), \dots$ are independent random variables:

$$P(N(A_1) = k_1 \wedge N(A_2) = k_2 \wedge \dots \wedge N(A_n) = k_n) = \prod_{i=1}^n P(N(A_i) = k_i). \quad (2)$$



Connectivity analysis

- One-connectivity probability $P(C)$ vs. node non-isolation probability $P(\bar{I})$
 - Node non-isolation is the necessary but non-sufficient condition of one-connectivity, thus $P(C) \leq P(\bar{I})$
 - Suppose the isolation of nodes to be independent events, we have:

$$\begin{aligned} P(\bar{I}) &= \sum_{k=0}^{\infty} P(\bar{I}|N = k) \cdot P(N = k) \\ &= \sum_{k=0}^{\infty} (1 - P(I))^k \cdot \frac{\lambda^k}{k!} e^{-\lambda} \\ &= e^{-\lambda P(I)} \sum_{k=0}^{\infty} \frac{[(1 - P(I))\lambda]^k}{k!} e^{-(1 - P(I))\lambda} \\ &= e^{-\lambda P(I)}. \end{aligned}$$



Connectivity analysis

- $P(I)$ is node isolation probability, D is node degree, D also follows Poisson distribution, we have:

$$P(I) = P(D = 0) = e^{-D_0}.$$

- D_0 can be calculated as

$$\begin{aligned} D_0 &= \rho \int_0^{2\pi} \int_0^{\infty} P(L|s) s ds d\phi \\ &= 2\pi\rho \int_0^{\infty} P(L|s) s ds. \end{aligned}$$

$$P(\bar{I}) = \exp(-\rho\|A\| \exp(-2\pi\rho \xi)), \quad \xi = \int_0^{\infty} P(L|s) s ds.$$



Link probability analysis

- Log-normal shadowing model

$$P_r(s) = P_t - PL(s_0) - 10\eta \log\left(\frac{s}{s_0}\right) + \mathcal{N}(0, \sigma),$$

- Incorporating anisotropic property

$$P_r(s) = P_t - (PL(s_0) + 10\eta \log\left(\frac{s}{s_0}\right)) \cdot K_i + \mathcal{N}(0, \sigma),$$

$$K_i = \begin{cases} 1, & \text{if } i = 0; \\ K_{i-1} + rand \cdot DOI, & \text{if } 0 < i < 360 \wedge i \in N, \end{cases}$$

$$DOI = 0.01821.$$



Link probability analysis

- PRR as a function of BER, taking NCFSK, Manchester encoding for example:

$$\Psi(\gamma) = (1 - \beta_M(\gamma))^{8(2f-h)}, \quad \beta_M = \frac{1}{2}e^{-\frac{\gamma}{2}}, \quad \gamma = 10^{\gamma_{dB}/10}.$$

$$\Psi(\gamma) = \left(1 - \frac{1}{2}e^{-\frac{\gamma}{2}}\right)^{8(2f-h)}.$$

- SNR can be obtained from the radio model

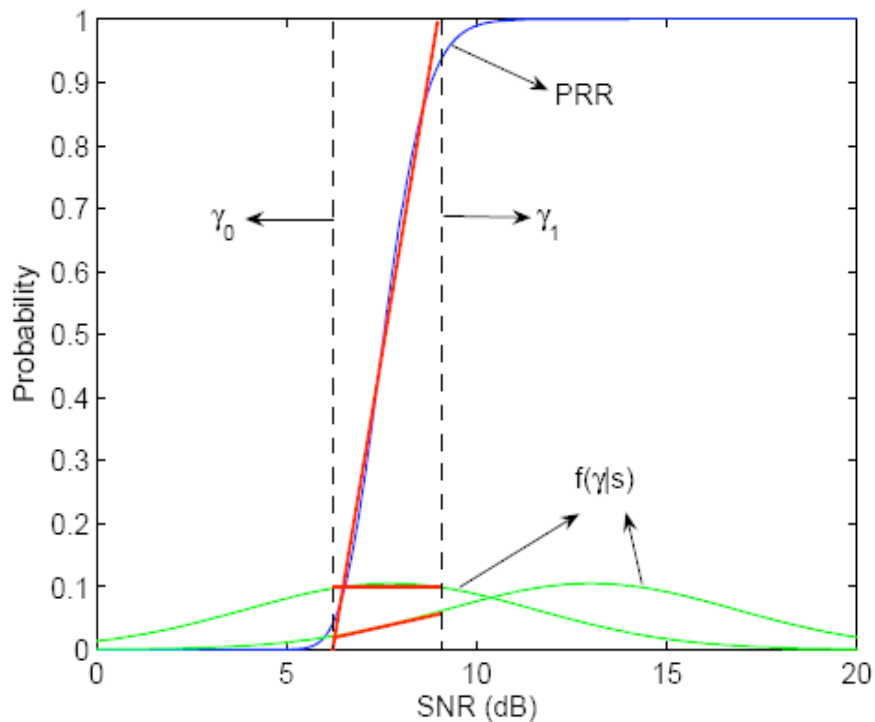
$$\gamma(s) = P_r(s) - P_n,$$

$$\mathcal{N}(\mu(s), \sigma) \quad \mu(s) = P_t - (PL(s_0) + 10\eta \log(\frac{s}{s_0})) \cdot K_i - P_n.$$

- Finally,

$$\xi = \int_0^\infty P(L|s) s ds = \int_0^\infty \int_{-\infty}^\infty \Psi(\gamma) f(\gamma|s) \cdot s d\gamma ds.$$

Link probability analysis



$$\Psi(\gamma) = \begin{cases} 0, & \gamma \leq \gamma_0; \\ k_\psi \gamma + b_\psi, & \gamma_0 < \gamma < \gamma_1; \\ 1, & \gamma > \gamma_1. \end{cases}$$

$$k_\psi = \frac{0.9 - 0.1}{\gamma_1 - \gamma_0}, b_\psi = \frac{0.1\gamma_1 - 0.9\gamma_0}{\gamma_1 - \gamma_0},$$

$$\gamma_0 = \Psi^{-1}(0.1), \gamma_1 = \Psi^{-1}(0.9).$$

$$f(\gamma|s) = k_f(s)\gamma + b_f(s), \quad \gamma \in [\gamma_0, \gamma_1],$$

$$k_f(s) = \frac{f(\gamma_1|s) - f(\gamma_0|s)}{\gamma_1 - \gamma_0}, \quad b_f(s) = \frac{f(\gamma_0|s)\gamma_1 - f(\gamma_1|s)\gamma_0}{\gamma_1 - \gamma_0}$$

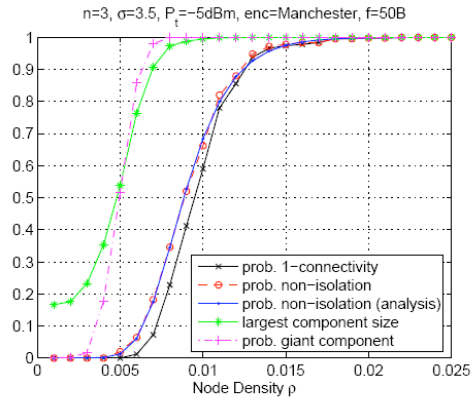
Link probability analysis

$$\begin{aligned}\xi &= \int_0^\infty \int_{-\infty}^\infty \Psi(\gamma) f(\gamma|s) \cdot s \, d\gamma \, ds \\ &\approx \int_0^\infty \int_{\gamma_0}^\infty \Psi(\gamma) f(\gamma|s) \cdot s \, d\gamma \, ds \\ &\approx \int_0^\infty \left(\int_{\gamma_0}^{\gamma_1} (k_\psi \gamma + b_\psi)(k_f(s)\gamma + b_f(s)) \, d\gamma + (1 - \Phi(\frac{\gamma_1 - \mu(s)}{\sigma})) \right) s \, ds \\ &\approx \int_0^\infty \int_{\gamma_0}^{\gamma_1} (k_\psi \gamma + b_\psi)(k_f(s)\gamma + b_f(s)) \cdot s \, d\gamma \, ds + \int_0^\infty (1 - \Phi(\frac{\gamma_1 - \mu(s)}{\sigma})) s \, ds \\ &\approx \int_0^{d_h} \int_{\gamma_0}^{\gamma_1} (k_\psi \gamma + b_\psi)(k_f(s)\gamma + b_f(s)) \cdot s \, d\gamma \, ds + \int_0^{d_h} (1 - \Phi(\frac{\gamma_1 - \mu(s)}{\sigma})) s \, ds,\end{aligned}$$

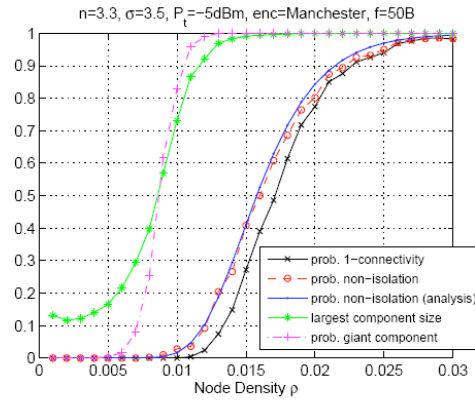


Simulation settings

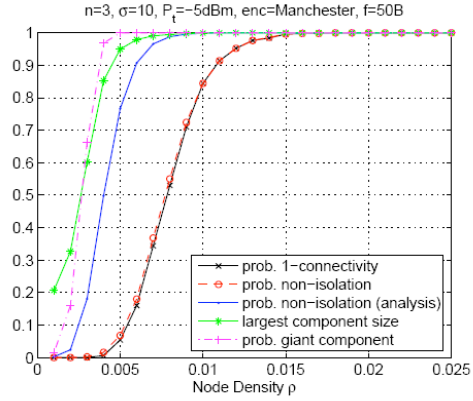
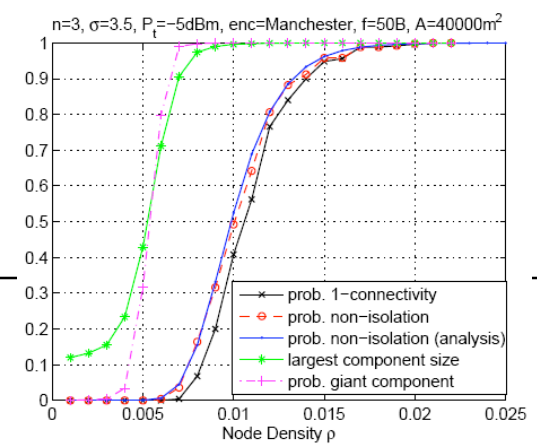
- Select a subarea, eliminating border effect
- Baseline: $n=3$, $\sigma=3.5$, $P_t=-5\text{dBm}$, encoding method=Manchester, frame size=50 bytes, $|A|=20000\text{m}^2$ (modulation=NCFSK)
- Comparison: theoretical-simulation results of non-isolation prob.; one-connectivity vs. non-isolation prob.; giant component vs. one-connectivity; impact of different parameters.



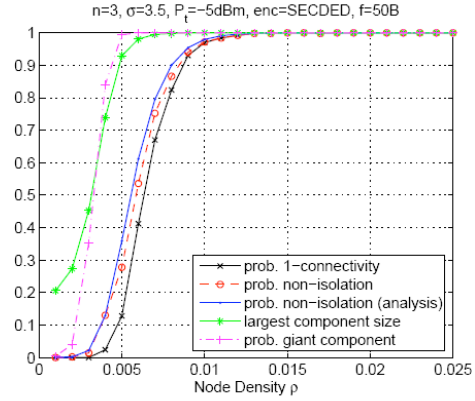
(a)



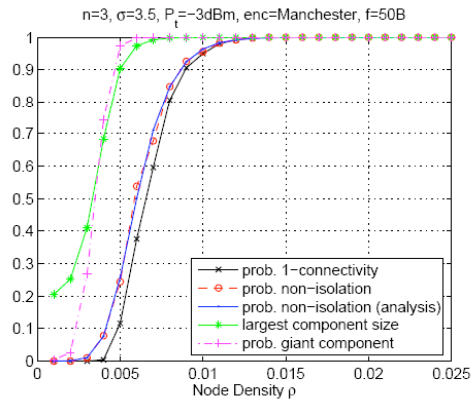
(b)



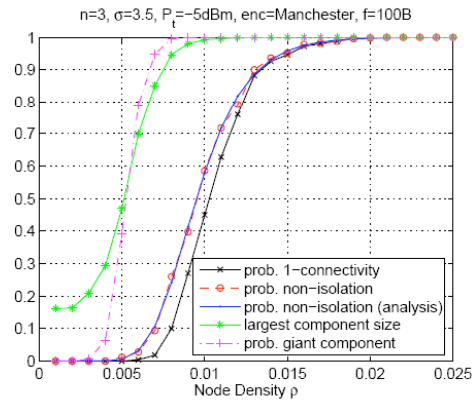
(c)



(d)



(e)



(f)



Discussion

- As node density increases, the transition from low connectivity and the appearance of giant component is quite sharp, which agree with the analysis using the theory of continuum percolation.
- Non-isolation probability serves as the upper bound of one-connectivity.

$$\rho(P(C) = p) = \rho(P(\bar{I}) = p) + \delta, \delta > 0. \text{ As } p \rightarrow 1, \delta \rightarrow 0.$$

When the shadowing variance gets large, the difference δ becomes smaller. This is because the increase of long links and the decrease of short links reduce the correlation between links. Thus the GRG approaches RG.



Discussion

- Theoretical performance of non-isolation probability matches simulated ones, except that when σ is large ($\sigma=10$). This is because network suffers severe link asymmetry as shadowing variance increase. The theoretical calculation overestimates the global connectivity performance.



Discussion

- The increase of pass loss exponent n shortens tx range; the increase in tx power increases the average tx range; impact of network size $|A|$ consists with the theoretical one.
- A different encoding scheme. SECDED (1:3) performs better than Manchester (1:2). Complicated encoding methods cost energy and memory space.
- Frame size change has a small influence



Discussion

- Giant component
 - For practical use, one-connectivity may be too stringent.
 - Giant component probability is defined as the largest component size larger than $N/2$.



Future work

- Temporal dynamics of wireless connectivity
- The giant component needs further analytical study
- K-connectivity



Major References

- Zuniga, M.; Krishnamachari, B. Analyzing the transitional region in low-power wireless links. In *Proc. IEEE SECON 2004*, 517–526.
- Zhou, G.; He, T.; Krishnamurthy, S.; Stankovic, JA. Models and solutions for radio irregularity in wireless sensor networks. *ACM Transaction on Sensor Networks* 2003, 2(2), 221–262.
- Bettstetter, C.; Hartmann, C. Connectivity of wireless multihop networks in a shadow fading environment. *Wireless Networks* 2005, 11(5), 571–579.
- Miorandi, D.; Altman, E. Coverage and connectivity of ad hoc networks presence of channel randomness. In *Proc. IEEE INFOCOM 2005*, 491–502.
- Bollobas, B. Random graphs. Cambridge University Press, 2001.



The end!

Thanks